J. Cell. Mol. Med. Vol 14, No 10, 2010 pp. 2436-2447

Vascular endothelial growth factor and substrate mechanics regulate *in vitro* tubulogenesis of endothelial progenitor cells

Donny Hanjaya-Putra, Jane Yee, Doug Ceci, Rachel Truitt, Derek Yee, Sharon Gerecht *

Department of Chemical and Biomolecular Engineering, Johns Hopkins Physical Science Oncology Center and Institute for NanoBio Technology, Johns Hopkins University, Baltimore, MD, USA

Received: July 24, 2009; Accepted: November 20, 2009

Abstract

Endothelial progenitor cells (EPCs) in the circulatory system have been suggested to maintain vascular homeostasis and contribute to adult vascular regeneration and repair. These processes require that EPCs break down the extracellular matrix (ECM), migrate, differentiate and undergo tube morphogenesis. Evidently, the ECM plays a critical role by providing biochemical and biophysical cues that regulate cellular behaviour. Using a chemically and mechanically tunable hydrogel to study tube morphogenesis *in vitro*, we show that vascular endothelial growth factor (VEGF) and substrate mechanics co-regulate tubulogenesis of EPCs. High levels of VEGF are required to initiate tube morphogenesis and activate matrix metalloproteinases (MMPs), which enable EPC migration. Under these conditions, the elasticity of the substrate affects the progression of tube morphogenesis. With decreases in substrate stiffness, we observe decreased MMP expression while increased cellular elongation, with intracellular vacuole extension and coalescence to open lumen compartments. RNAi studies demonstrate that membrane type 1-MMP (MT1-MMP) is required to enable the movement of EPCs on the matrix and that EPCs sense matrix stiffness through signalling cascades leading to the activation of the RhoGTPase Cdc42. Collectively, these results suggest that coupled responses for VEGF stimulation and modulation of substrate stiffness are required to regulate tube morphogenesis of EPCs.

Keywords: extracellular matrix • endothelial progenitor cells • angiogenesis • vascular endothelial growth factor • tubulogenesis

Introduction

In recent decades, postnatal vasculogenesis has been considered to be an important mechanism for neovascularization *via* circulating endothelial progenitor cells (EPCs) derived from marrow [1, 2]. Since then, EPCs have been proposed as a potential therapeutic tool for treating vascular disease, either through infusion to the site of vascularization [3, 4] or *ex vivo* expansion for engineering vascularized tissue constructs [5, 6]. Understanding the molecular mechanism that regulates neovascularization by EPCs will provide insights for therapeutic vascularization.

Differentiation, mobilization and recruitment of EPCs and endothelial cells (ECs) have been established to be regulated foremost by vascular endothelial growth factor (VEGF) [7, 8]. Administration of VEGF into the site of ischemia has been reported to induce ECs mobilization and restore blood flow [9, 10]. The extracellular matrix (ECM) provides critical support for ECs; their adhesion to the ECM is required for their proliferation, migration, morphogenesis and survival – as well as, ultimately, for the stabilization of blood vessels [11] – through both biochemical and mechanical functions [12–14]. Matrix elasticity has been reported to induce stem cell differentiation and morphological changes [15, 16]. Changes in physical interactions between cell surface integrins and the ECM, due to alterations in ECM elasticity, regulate cell shape and cytoskeletal structure [17–19]. Mechanical forces exerted by ECs on the matrix stimulate capillary growth *in vivo* [20] and formation of capillary-like structures (CLSs) *in vitro* [21, 22]. Recently, matrix elasticity has been reported to modulate the expression of VEGF receptor 2 (VEGFR2) [14], and biomechanical forces alone were sufficient to mediate vascular growth *in vivo* independent of endothelial sprouting [23].

Tube morphogenesis is essential for the development of a functional circulatory system [24, 25]. Longitudinal vacuoles that appeared to be extruded and connected from one cell to the next were first described by Folkman and Haudenschild [26]. These observations were confirmed and extended by later studies showing that intracellular vacuoles arise from events downstream of

*Correspondence to: Sharon GERECHT,
Department of Chemical and Biomolecular Engineering, Johns Hopkins Physical Science Oncology Center and Institute for NanoBio Technology, Johns Hopkins University, 3400 N. Charles St.,
Baltimore, MD, 21218, USA.
Tel.: 410–516-2846
Fax: 410–516-5510
E-mail: gerecht@jhu.edu

doi:10.1111/j.1582-4934.2009.00981.x

integrin–ECM signalling interactions, where lumen formation is mediated through the activation of the Rho GTPase Cdc42 [25, 27–29]. Moreover, at the site of neovascularization, activated membrane type 1-matrix metalloproteinase (MT1-MMP) activates pro-MMPs at the pericellular area, which digest the ECM and allow EC migration and tubulogenesis [30, 31]. Such matrix remodelling by MMPs is implicated in various pathological conditions including atherosclerosis, inflammation, and ischemia [32, 33].

Here, we utilized hydrogels with defined composites and tunable elasticity for *in vitro* studies of tube morphogenesis. These hydrogels served as substrates of varying stiffnesses, allowing us to study the kinetics of EPC tubulogenesis. Viscoelasticity measurements during *in situ* gelation demonstrated three distinct substrate stiffness profiles: rigid, firm and yielding. We first demonstrated that, while low levels of VEGF allowed EPCs to spread on all substrates, high levels of VEGF were required to initiate tube morphogenesis and to activate MMPs, whose expression declined with the decrease of matrix stiffness. We then observed that increased tube morphogenesis – including CLS progression, vesicle formation, expansion (in both size and number) and fusion to lumens – corresponded to decreased substrate rigidity. RNA interference (RNAi) studies further showed that EPCs required MT1-MMP and Cdc42 to undergo tube morphogenesis.

Materials and methods

Human EPCs

Human umbilical cord EPCs isolated from outgrowth clones, kindly provided by Dr. Yoder, Indiana University School of Medicine, were expanded and used for experiments between passages 3 and 10. For the current study, EPCs were isolated from seven healthy newborns (three females and four males; gestational age range, 38–40 weeks), pooled, expanded and characterized according to previously established protocol by Yoder and colleagues [34–38]. Briefly, EPCs were expanded in flasks coated with type I collagen (Roche Diagnostics, Basel, Switzerland), in endothelial growth medium (EGM; PromoCell, Heidelberg, Germany) supplemented with 1 ng/ml $VEGF_{165}$ (Pierce, Rockford, IL, USA), and incubated in a humidified incubator at 37°C in an atmosphere containing 5% CO_2. EPCs were passaged every 3 to 4 days with 0.05% trypsin (Invitrogen, Carlsbad, CA, USA) and characterized for the positive expression of cell-surface antigens CD31, CD141, CD105, CD144, vWF and Flk-1, and the negative expression of hematopoietic-cell surface antigens CD45 and CD14. Single cell colony forming assays were used to characterize their robust proliferative potential, secondary and tertiary colony formation upon replating.

Preparation of hyaluronic acid (HA)-gelatin hydrogels

HA-gelatin hydrogels (Extracel, Glycosan BioSystems, Inc., Salt Lake City, UT, USA) were prepared as previously described [39]. Briefly, the hydrogels were obtained by mixing 0.4% (w/v) Glycosil solution with 0.4% (w/v) Gelin-S solution in a 1:1 volume ratio with 1%, 0.4% and 0.1% (w/v) of polyethylene glycol diacrylate (PEGDA) crosslinker (MW 3400) in a 4:1 volume ratio, to obtain rigid, firm and yielding substrates, respectively. The pregel solution was cast into a 96-well glass bottom plate (MatTek, Ashland, MA, USA) for live/dead assay and CLS quantification and a 16-well Lab-Tek chamber slide (NUNC, Rochester, NY, USA) for transmission electron microscopy (TEM) analysis and confocal images. After gelation, all hydrogels were allowed to cure for 12 hrs inside a biological safety cabinet to stabilize PEGDA-mediated crosslinking.

Viscoelasticity measurement

Oscillatory shear measurements of the elastic modulus (G′) were obtained using a constant strain rheometer with steel cone-plate geometry (25 mm in diameter; RFS3, TA Instruments, New Castle, DE, USA) as previously described [39]. Briefly, oscillatory time sweeps were performed on three samples ($n = 3$) for stiff, rigid and yielding hydrogels to monitor the *in situ* gelation. The strain was maintained at 20% during the time sweeps by adjusting the stress amplitude at a frequency of 1 Hz. This strain and frequency were chosen because G′ was roughly frequency independent within the linear viscoelastic regime. The 24-hr tests occurred in a humidified chamber at a constant temperature (25°C) in 30-sec. intervals. The Young's modulus (substrate stiffness) was calculated by $E = 2G'(1 + \nu)$ HA-gelatin hydrogels can be assumed to be incompressible [39], such that their Poisson's ratios (ν) approach 0.5 and the relationship becomes $E = 3G'$ [14, 40].

Angiogenesis assay

CB EPCs were seeded on rigid, firm and yielding substrates, cured for 12 hrs, with densities of 100,000 cells/cm^2. Constructs were cultured for 12 hrs in EGM (PromoCell GmbH, Heidelberg, Germany) supplemented with 1, 10, 25 or 50 ng/ml recombinant human $VEGF_{165}$ (Pierce). Visualization and image acquisition were performed with an inverted light microscope (Olympus IX50, Center Valley, PA, USA) at time intervals of 3, 6, 9 and 12 hrs.

Quantification of CLSs

The LIVE/DEAD Viability/Cytotoxicity Kit (Invitrogen) was used to visualize CLSs, following the manufacturer's protocol. Briefly, calcein AM dye was diluted in phenol red-free DMEM (Invitrogen) to obtain a final concentration of 2 μM. The constructs were incubated with the dye solution for 30 min. After replacing with fresh phenol red-free DMEM, CLSs were visualized using a fluorescent microscope with a 10× objective lens (Axiovert, Carl Zeiss, Inc., Thornwood, NY, USA). We analysed four image fields per construct from three distinct experiments ($n = 3$) performed in triplicate, using Metamorph software 6.1 (Universal Imaging Co., Downingtown, PA, USA) to quantify and compare CLSs formed on each substrate.

Immunofluorescence

EPCs cultured on hydrogels for 12 hrs were fixed using formalin-free fixative (Accustain, Sigma-Aldrich, St. Louis, MO, USA) for 20 min., and washed with PBS. For staining, cells were permeabilized with a solution of

0.1% Triton-X for 10 min., washed with PBS and incubated for 1 hr with mouse anti-human VE-Cad (1:200; BD Biosciences, San Jose, CA, USA), rinsed twice with PBS and incubated with antimouse IgG Cy3 (1:50; Sigma, St. Louis). After rinsing twice with PBS, cells were incubated with either FITC-conjugated lectin (1:40, Vector, Burlingame, CA, USA) or FITC-conjugated phalloidin (1:40, Molecular Probes, Eugene, OR, USA) for 1 hr, rinsed with PBS and incubated with DAPI (1:1000; Roche Diagnostics) for an additional 10 min. The hydrogels were gently placed into a glass bottom dish (MaTek, Ashland, MA, USA) and mounted with fluorescent mounting medium (Dako, Glostrup, Denmark). The immunolabelled cells were examined using fluorescence microscopy (Olympus BX60). A sequence of *z*-stack images was obtained using confocal microscopy (LSM 510 Meta, Carl Zeiss, Inc.).

Transmission electron microscopy

EPCs cultured on hydrogels for 6 and 12 hrs were prepared for TEM samples as previously described [41]. Briefly, cells were fixed with 3.0% formaldehyde, 1.5% glutaraldehyde in 0.1 M Na cacodylate, 5 mM Ca^{2+} and 2.5% sucrose at room temperature for 1 hr and washed three times in 0.1 M cacodylate/2.5% sucrose pH 7.4 for 15 min. each. The cells were post-fixed with Palade's OsO_4 on ice for 1 hr, rinsed with Kellenberger's uranyl acetate and then processed conventionally through Epon embedding on a 16-well Lab-Tek chamber slide (NUNC). Serial sections were cut, mounted onto copper grids and viewed using a Phillips EM 410 transmission electron microscope (FEI, Hillsboro, OR, USA). Images were captured with an FEI Eagle 2k camera.

RNAi transfection

EPCs were transfected with siGENOME SMARTpool human Cdc42 and MT1-MMP (Dharmacon, Lafayette, CO, USA) using the manufacturer's protocol. Briefly, the RNAi transfection solution was prepared by mixing a serum-free and antibiotic-free EGM (PromoCell GmbH) with DharmaFECT2 RNAi transfection reagent (Dharmacon). EPCs were cultured to 90% confluency on a 24-well plate (NUNC, Roskilde, Denmark). For transfection, EPC growth medium was removed and replaced with 400 μl of antibiotic-free EGM (PromoCell) and 100 μl transfection solution in each well, to achieve a final RNAi concentration of 50 nmol/l. Transfected cells were incubated at 37°C, and the medium was replaced with a fresh EGM medium after 24 hrs. RNA analysis was performed after 48 hrs, and protein analysis was performed after 72 hrs. Confirmed transfected EPCs were used for experiments after 48 to 96 hrs.

Real-time RT-PCR

Two-step RT-PCR was performed on EPCs cultured in media supplemented with 1 ng/ml or 50 ng/ml VEGF. Total RNA was extracted using TRIzol (Gibco, Invitrogen Co., Carlsbad, CA, USA) according to the manufacturer's instructions. Total RNA was quantified by an ultraviolet spectrophotometer, and the samples were validated for no DNA contamination. RNA (1 μg per sample) was reversed transcribed using M-MLV (Promega Co., Madison, WI, USA) and oligo(dT) primers (Promega Co.) according to the manufacturer's instructions. We used the TaqMan Universal PCR Master Mix and Gene Expression Assay (Applied Biosystems, Foster City, CA, USA) for *MMP-1*, *MMP-2*, *MT1-MMP*, *HPRT1* and β-ACTIN, according to the manufacturer's instructions. The TaqMan PCR step was performed in triplicate with an Applied Biosystems StepOne Real-Time PCR system (Applied Biosystems), using the manufacturer's instructions. The relative expression of *MMP1*, *MMP2* and *MT1-MMP* was normalized to the amount of *HPRT1* or *β-ACTIN* in the same cDNA by using the standard curve method described by the manufacturer. For each primer set, the comparative CT method (Applied Biosystems) was used to calculate amplification differences between the different samples. The values for experiments ($n = 3$) were averaged and graphed with standard deviations. Similar procedures were used to analyse the expressions of Cdc42 and MT1-MMP from the RNAi experiments.

Western blot

The relative amounts of MT1-MMP or Cdc42 in RNAi transfected EPCs were detected using Western blotting of whole cell lysates prepared in standard extraction buffer containing 4% SDS, 20% glycerine and 0.0125 M Tri-HCl pH 6.8. Protein (20 μg) from these samples was separated in a 12.5% Criterion Tris-HCl Gel (Bio-Rad Lab., Hercules, CA, USA) for 40 min. using Tris/glycine/SDS running buffer. Resolved proteins were transferred to immuno-blot nitrocellulose membranes (Bio-Rad Lab) and blocked with 3% dry-milk in Tris buffered saline-tween. The membranes were immunoprobed overnight with anti-human rabbit monoclonal antibodies to MT1-MMP (1:1000, Epitomics, Burllingame, CA, USA) and to Cdc42 (1:1000, Cell Signaling Technology, Beverly, MA, USA). For loading control, the membranes were probed with anti-human mouse beta-Actin (1:1000, Cell Signaling Technology). Next, membranes were treated with either HRP-conjugated anti-rabbit or antimouse IgG secondary antibodies (1:1000, Cell Signaling Technology) and then developed by adding SuperSignal West Pico Chemiluminescent Substrate (Thermo Scientific Pierce, Rockford, IL, USA).

Statistical analysis

Statistical analysis of CLSs quantification, MMP productions and RNAi suppression data was performed with GraphPad Prism 4.02 (GraphPad Software Inc., La Jolla, CA, USA). Parametric two-way ANOVA tests were performed to assess the significance of MMP production by EPCs among rigid, firm and yielding substrates cultured in low and high VEGF concentrations. Unpaired Student's t-tests were performed to analyse CLSs quantification and RNAi suppression data. Significance levels were set at $^{*}P < 0.05$, $^{**}P < 0.01$ and $^{***}P < 0.001$, respectively.

Results

Mechanically tunable matrix for *in vitro* tube morphogenesis

In this study, we used HA-based hydrogels to study EPC tube morphogenesis. One advantage of HA hydrogels is that the chemistry of the network is easily controlled *via* reaction conditions and is uniform between the various batches, which is difficult or impossible to achieve with naturally derived matrices such as matrigel and collagen. Furthermore, while enzymatic crosslinking of such natural gels as matrigel and collagen allows studies of increased stiffness, chemically modified HA-based hydrogels enable control

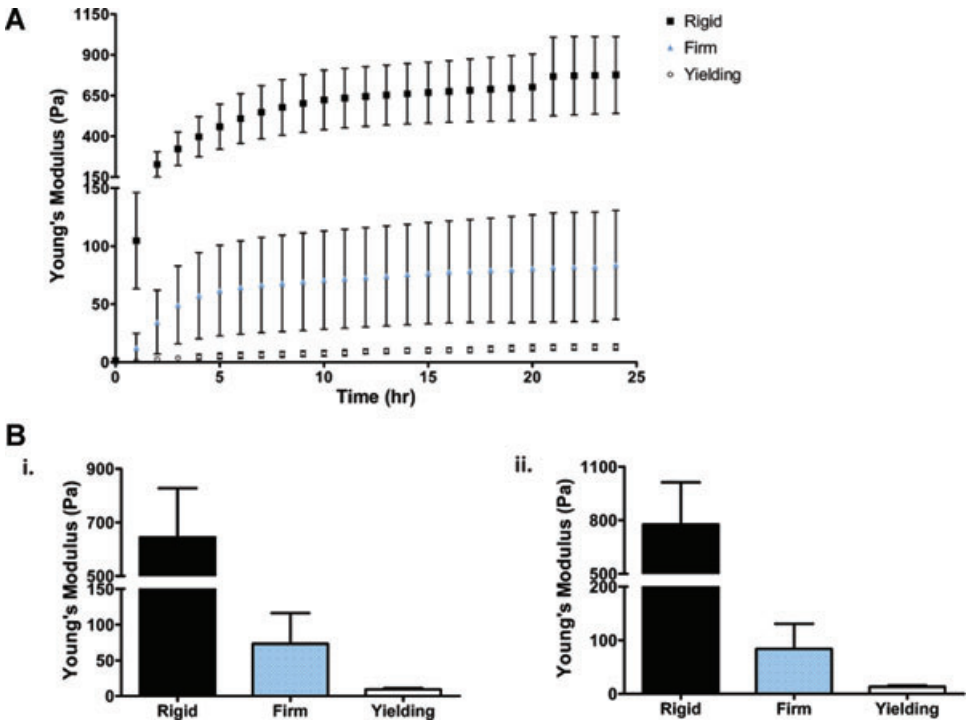

Fig. 1 Viscoelasticity of hydrogels. (**A**) Microrheology measurements of HA:gelatin in a 1:1 volume ratio with 1%, 0.4% and 0.1% (w/v) of PEGDA crosslinker over 24 hrs of gelation show three distinct profiles of hydrogel mechanics: rigid, firm and yielding. Values shown are means ± S.D. for Young's modulus (E) over 24 hrs during the *in situ* gelation (please see Fig. S1 for elastic modulus (G′) data). (**B**) (*i*) After 12 hrs, the values of Young's modulus (stiffness) were: 650 ± 180 Pa for rigid hydrogel, 75 ± 40 Pa for firm hydrogel, and 10 ± 2 Pa for yielding hydrogel. (*ii*) After an additional 12-hr gelation period, a slight increase in stiffness was observed in all three hydrogels with values of: 780 ± 240 Pa, 85 ± 40 Pa and 15 ± 3 Pa, respectively.

over crosslinking density, thus offering an opportunity to study cellular responses to a wide range of tunable mechanical stimuli. Previous studies demonstrated that HA-based hydrogels support *in vivo* angiogenesis [42] and embryonic vasculogenesis [43]. For the present study, we utilized thiol-modified HA-gelatin hydrogels to enable EPC attachment. These hydrogels can be mechanically tuned using the PEGDA crosslinker while preserving uniform presentation of cell adhesion molecules [39]. In the first stage, we generated different hydrogels with the same HA:gelatin ratio, but with increased PEGDA crosslinker concentration, and examined the gelation kinetics (Fig. 1). We showed that within 12 hrs of hydrogels curing, distinct Young's modulus (stiffness) profiles were established for rigid (650 Pa), firm (75 Pa) and yielding (10 Pa) hydrogels. After an additional 12 hrs of gelation, we observed a slight increase in stiffness for all hydrogels (rigid to 780 Pa, firm to 85 Pa and yielding to 15 Pa). The 24-hr gelation period was sufficient to completely crosslink all available thiol groups on the hydrogels at this HA:gelatin and PEGDA crosslinker composition [39]. Indeed, further gelation time did not significantly increase substrate stiffness (data not shown). We therefore chose to cure HA hydrogels for 12 hrs, and used the 12- to 24-hr period during which hydrogel mechanics are fairly constant to analyse EPC tube morphogenesis.

Effect of VEGF on *in vitro* tube morphogenesis

Cord blood-derived EPCs were demonstrated to form functional and stable blood vessels *in vivo* compared to adult peripheral blood EPCs, which formed blood vessels that were unstable and that regressed rapidly [44]. We previously used EPCs to study *in vitro* capillary tube formation induced by substrate nanotopography [45]. *In vitro* tube morphogenesis with lumen compartments was established as a prerequisite to define CB-EPCs [38, 46]. Therefore, to study tube morphogenesis in a controllable *in vitro* system, we seeded EPCs on HA hydrogel substrates cured for 12 hrs in media supplemented with either 1 ng/ml (low) or 50 ng/ml (high) VEGF. High concentrations of VEGF (*i.e.* 50 ng/ml) were previously demonstrated to induce vascular differentiation of embryonic stem cells [47] and vasculogenesis in HA hydrogels [43]. After 12 hrs of incubation, no tube formation was observed in any culture supplemented with 1 ng/ml VEGF, while some extent of CLS formed on the rigid and firm substrates, and predominant CLSs, similar to the CLSs observed on matrigel, formed on the yielding substrate supplemented with 50 ng/ml VEGF (Fig. 2A). To examine whether VEGF would induce MMP production, real time RT-PCR was performed to compare MMP expression in EPCs cultured on rigid, firm and yielding substrates supplemented with high VEGF, to their counterparts cultured with low VEGF. After 12 hrs of incubation in media supplemented with high VEGF, EPCs cultured on all substrate showed increased production of MMPs. Specifically, EPCs cultured on rigid and firm substrates with high VEGF produced three times the MMP-2 and four times the MMP-1 and MT1-MMP produced by EPCs cultured in media supplemented with low VEGF concentration. EPCs cultured on yielding substrate supplemented with high VEGF showed a smaller, but significant, increase in MT1-MMP, MMP-1 and MMP-2 compared

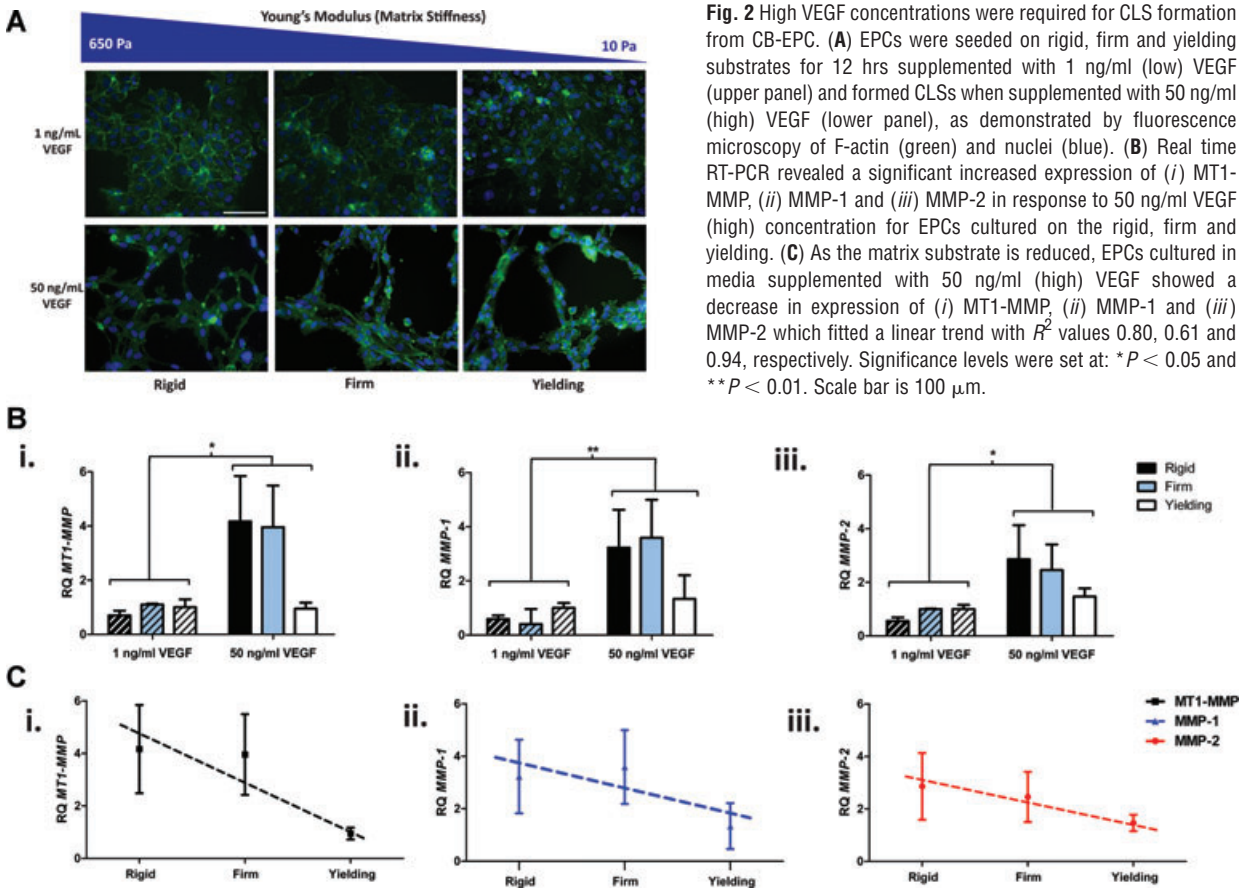

Fig. 2 High VEGF concentrations were required for CLS formation from CB-EPC. (**A**) EPCs were seeded on rigid, firm and yielding substrates for 12 hrs supplemented with 1 ng/ml (low) VEGF (upper panel) and formed CLSs when supplemented with 50 ng/ml (high) VEGF (lower panel), as demonstrated by fluorescence microscopy of F-actin (green) and nuclei (blue). (**B**) Real time RT-PCR revealed a significant increased expression of (*i*) MT1-MMP, (*ii*) MMP-1 and (*iii*) MMP-2 in response to 50 ng/ml VEGF (high) concentration for EPCs cultured on the rigid, firm and yielding. (**C**) As the matrix substrate is reduced, EPCs cultured in media supplemented with 50 ng/ml (high) VEGF showed a decrease in expression of (*i*) MT1-MMP, (*ii*) MMP-1 and (*iii*) MMP-2 which fitted a linear trend with R^2 values 0.80, 0.61 and 0.94, respectively. Significance levels were set at: $^*P < 0.05$ and $^{**}P < 0.01$. Scale bar is 100 μm.

to their counterpart cultured in low VEGF concentration (Fig. 2B). Interestingly, we noticed that when EPCs were cultured in media supplemented with high VEGF concentration, the MMP production decreases as the stiffness of the substrate was reduced (Fig. 2C). It should be noted that intermediate VEGF concentrations (*e.g.* 10 ng/ml or 25 ng/ml) increased tube morphogenesis on all substrates compared to 1 ng/ml, but with inferior outcomes when compared to high VEGF concentrations (data not shown). We therefore continued our studies of tube morphogenesis using high concentrations of VEGF.

Effect of substrate mechanics on *in vitro* tube morphogenesis

To study the kinetics of tube morphogenesis on substrates with different mechanics, we analysed the following parameters: (*i*) CLS phenotype; (*ii*) EPC layering and lengthening and, (*iii*) cytoplasmic vacuole formation, extension and fusion to open lumen compartments. EPCs were seeded on rigid, firm and yielding substrates in media containing high VEGF concentrations. Time-interval images show that EPCs assembled in a chain in an efficient and rapid manner on softer substrates (Fig. S2), resulting in a significant increase in tube length – from 130 ± 3 μm on rigid substrate to 140 ± 4 μm on firm substrate to 200 ± 5 μm on yielding substrate. Similarly, the area covered by CLSs also increased – from 560 ± 10 μm^2 on rigid substrate to 630 ± 24 μm^2 on firm substrate to 1011 ± 66 μm^2 on yielding substrate (Fig. 3A). Although the extent of CLSs that formed on all of the substrates increased over time, with further incubation the extent of CLSs that formed on rigid and firm substrates did not achieve the predominance of CLSs that formed on yielding substrate (data not shown). In addition, CLSs that formed on yielding substrate were further found to be considerably thicker (20 ± 1 μm) than those that formed on either rigid (17 ± 1 μm) or firm (18 ± 0.3 μm) substrates, with branching and visible hollowing indicative of tubular structure with open lumen space (Fig. 3B).

To investigate the kinetics of cytoplasmic vesicle formation, coalescing and elongation to an open lumen, TEM analysis was performed after 6 and 12 hrs of culture. After 6 hrs, cytoplasmic vacuoles were observed in EPCs cultured on all substrates. However, while EPCs on rigid substrate were organized into two to three cell layers, they elongated on firm substrate and both elongated and organized into a single layer on the yielding substrate (Fig. 4A). After 12 hrs of culturing, EPCs on rigid substrate were more elongated and contained many vacuoles. On firm substrate, cells were elongated with larger

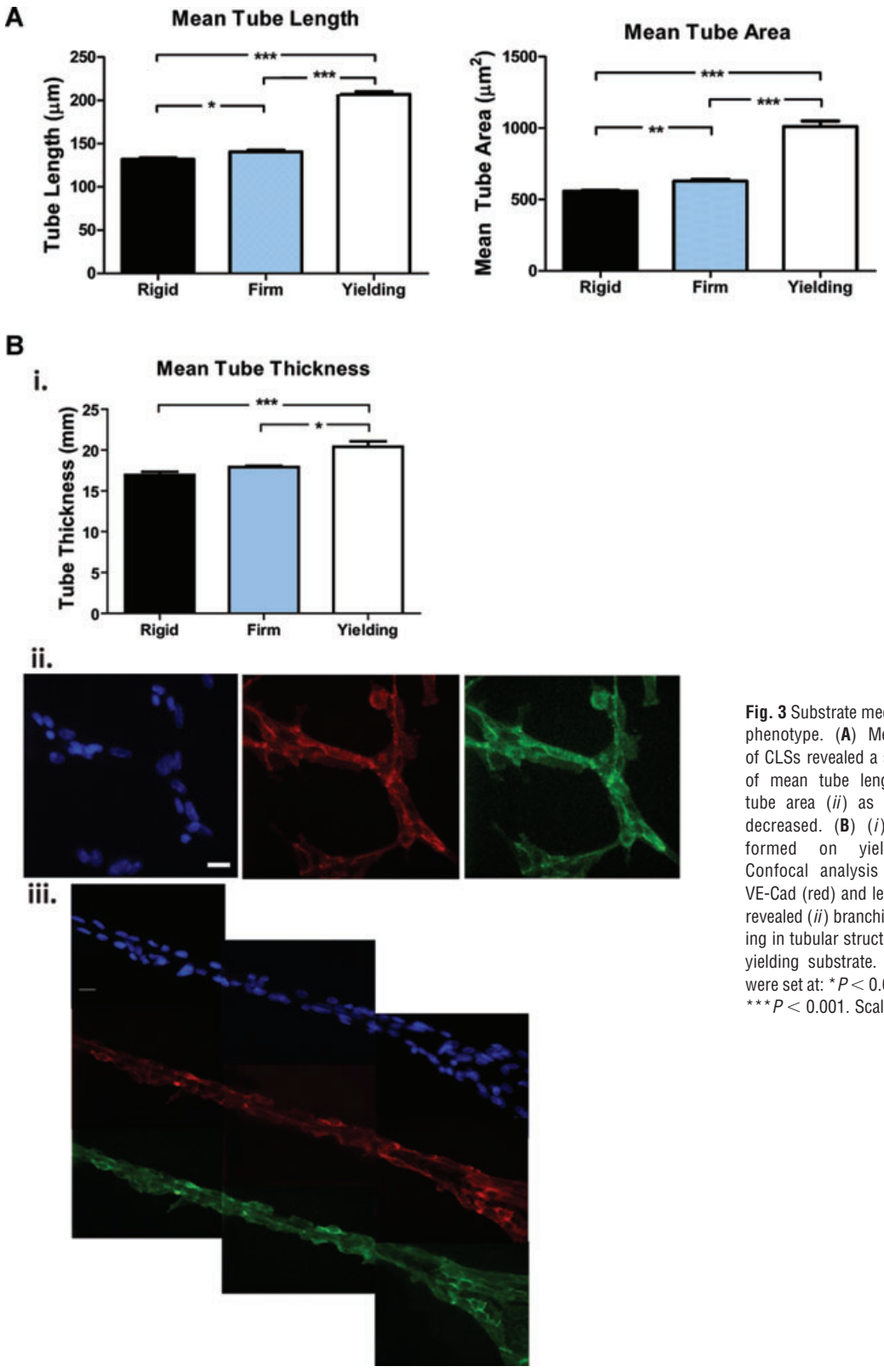

Fig. 3 Substrate mechanics affects CLS phenotype. (**A**) Metamorph analysis of CLSs revealed a significant increase of mean tube length (*i*) and mean tube area (*ii*) as substrate stiffness decreased. (**B**) (*i*) Thickened CLSs formed on yielding substrates. Confocal analysis of nuclei (blue), VE-Cad (red) and lectin (green) further revealed (*ii*) branching and (*iii*) hollowing in tubular structures formed on the yielding substrate. Significance levels were set at: $^{*}P < 0.05$, $^{**}P < 0.01$ and $^{***}P < 0.001$. Scale bars are 20 μm.

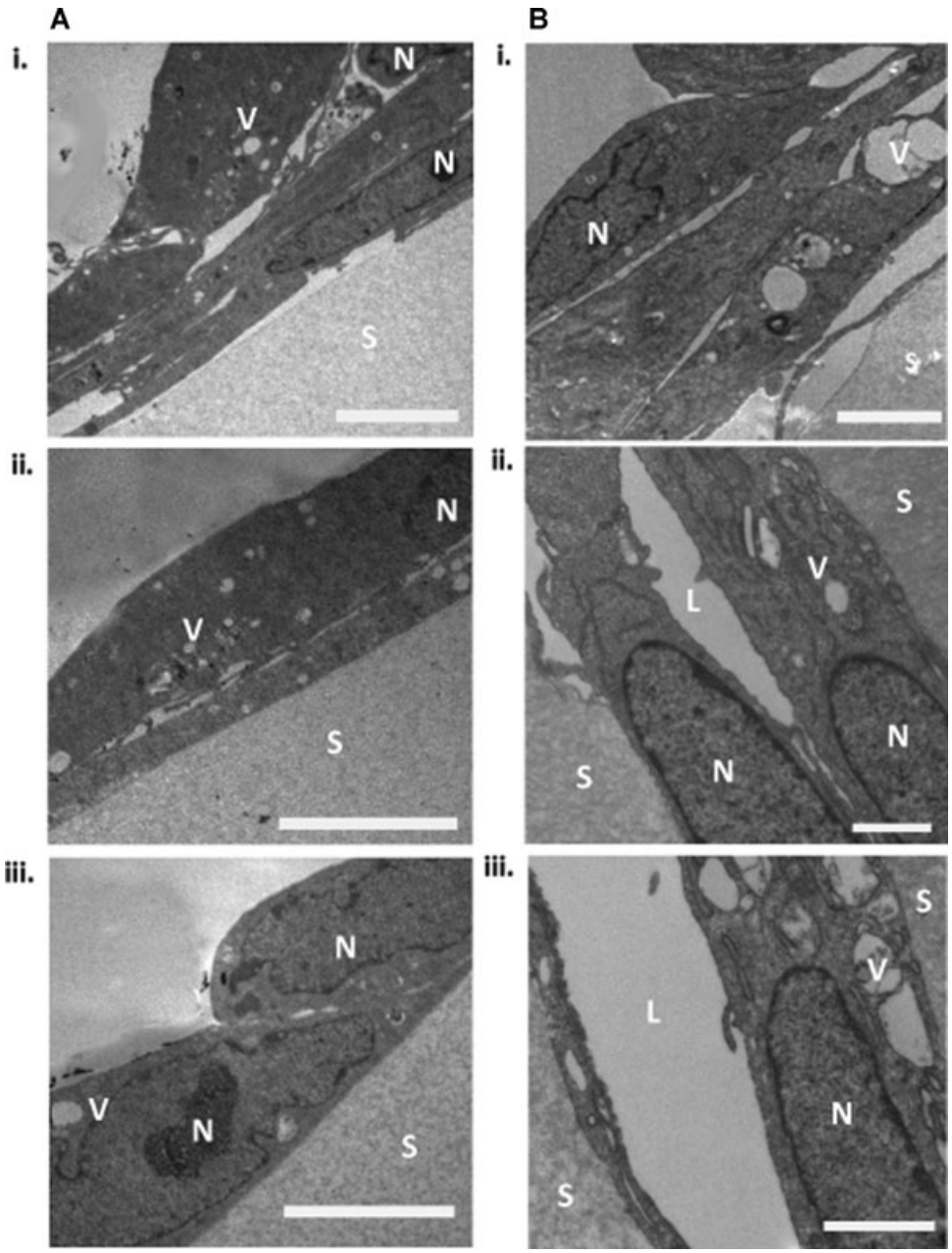

Fig. 4 Substrate mechanics regulates vacuole and lumen formation. (**A**) TEM analyses of CLSs formed after 6 hrs showed vacuoles (V) forming on all substrates (S), while EPCs formed two to three layers on rigid substrate, extended on firm substrate and formed an elongated single layer on yielding substrates. (**B**) After 12 hrs, EPCs grew longer on all substrates and contained many vacuoles (V) on rigid substrate (S), enlarged vacuoles with occasionally noted lumens (L) on firm substrate, and open lumens (L) in complex, lengthened cellular structures on yielding substrates. Cell nucleus is indicated in N. Scale bars are 10 μm in (**A**) and 2 μm in (**B**).

vacuoles, and lumen compartments were observed on several occasions. On yielding substrate, we observed complex structures with open lumen spaces and very lengthened cells (Fig. 4B).

MT1-MMP and Cdc42 required for *in vitro* tube morphogenesis

MT1-MMP has been reported to support neovascularization by allowing matrix degradation at the migrating cell front [48], as well as by creating a physical space to control tube and lumen morphogenesis [49, 50]. To examine the function of MT1-MMP in tube morphogenesis of EPCs on various levels of substrate stiffness, we utilized an RNAi suppression approach. EPCs treated with siRNA targeting the MT1-MMP (Fig. S3) were seeded on the different substrates. In contrast to the Luciferase-treated EPCs (control), siRNA suppression of MT1-MMP mitigated CLS formation on firm and yielding substrates, with more rounded cell morphology, while allowing cell spreading on rigid substrates (Figs. 5 and S3).

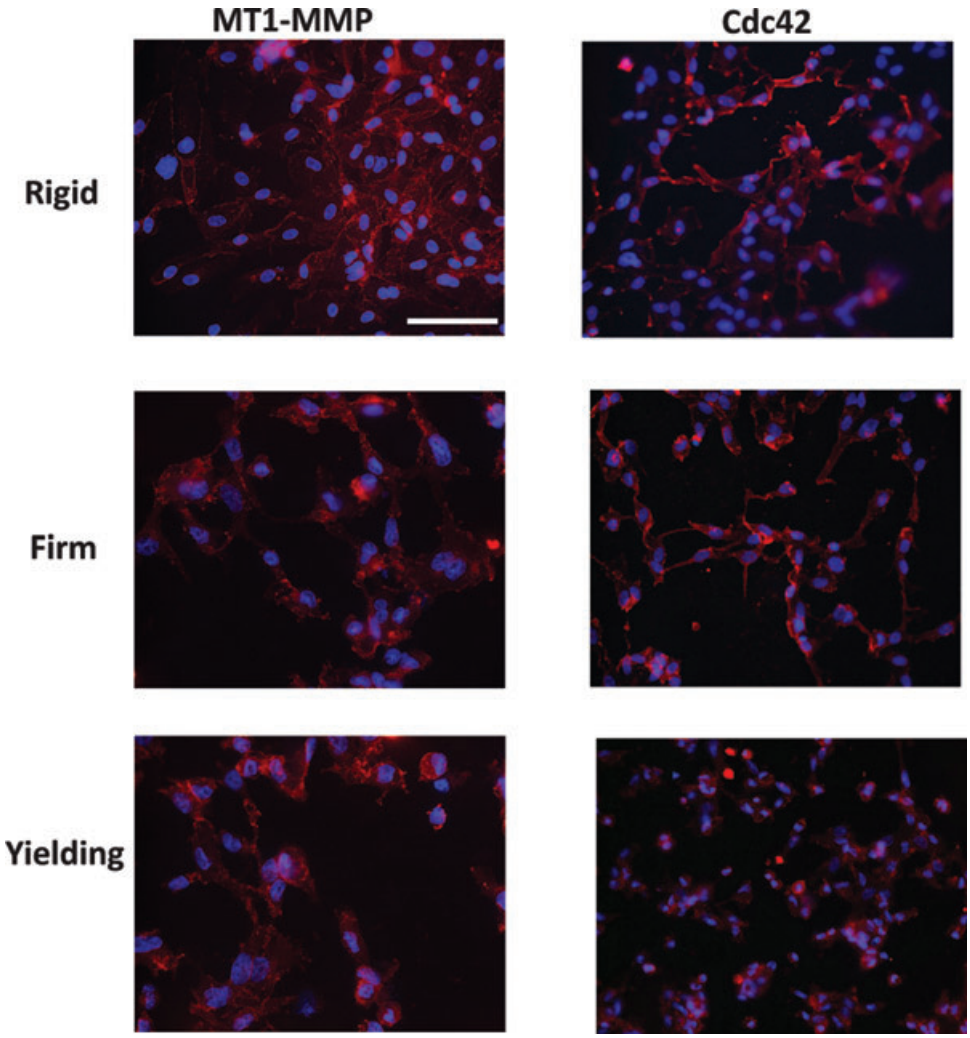

Fig. 5 MT1-MMP and Cdc42 required for CLS formation from EPC. EPCs transfected with the indicated siRNA were seeded on rigid, firm and yielding substrates and supplemented with 50 ng/ml VEGF for 12 hrs with no indication of CLS formation as demonstrated by fluorescence microscopy of VE-cad (red) and nuclei (blue). Scale bar is 100 μm.

Cdc42 has been demonstrated to regulate EC morphogenesis through vacuole and lumen formation [27], as well as to mediate cell spreading, motility, growth and differentiation through cytoskeletal remodelling and focal adhesion assembly [51, 52]. We utilized an RNAi suppression approach to examine whether Cdc42 is the connecting link by which EPCs respond to substrate stiffness during tube morphogenesis. EPCs were treated with siRNA that targeted the small Rho GTPase Cdc42 (Fig. S3) and were seeded on the different substrates. Luciferase-treated (control) EPCs were able to spread and form some extent of CLSs on rigid and firm substrates and could form CLSs to a greater extent on yielding substrate. However, siRNA suppression of Cdc42 prevented EPC tube morphogenesis on all substrates; we observed rounded cell morphology on the yielding substrate and a more spreading morphology on the rigid and firm substrates (Figs. 5 and S3).

Discussion

Postnatal vasculogenesis has been considered to be an important mechanism for angiogenesis *via* marrow-derived circulating EPCs [1]. In response to VEGF, EPCs are mobilized to the site of vascularization, which initiates their proliferation and differentiation [53]. After activation, EPCs undergo a complex process that involves migration, digestion of basement membrane, sprouting, tube morphogenesis and ultimately, blood vessel stabilization [11, 54]. The ECM components play an important role in these cascades of events, which are also regulated by cytokines, integrins and proteases. Therefore, changes in ECM mechanics may modulate properties of EPCs.

Changes in ECM mechanics can lead to focal changes in growth factor availability, can guide developmental and adaptive changes, and can affect cellular fate and the lineage commitment

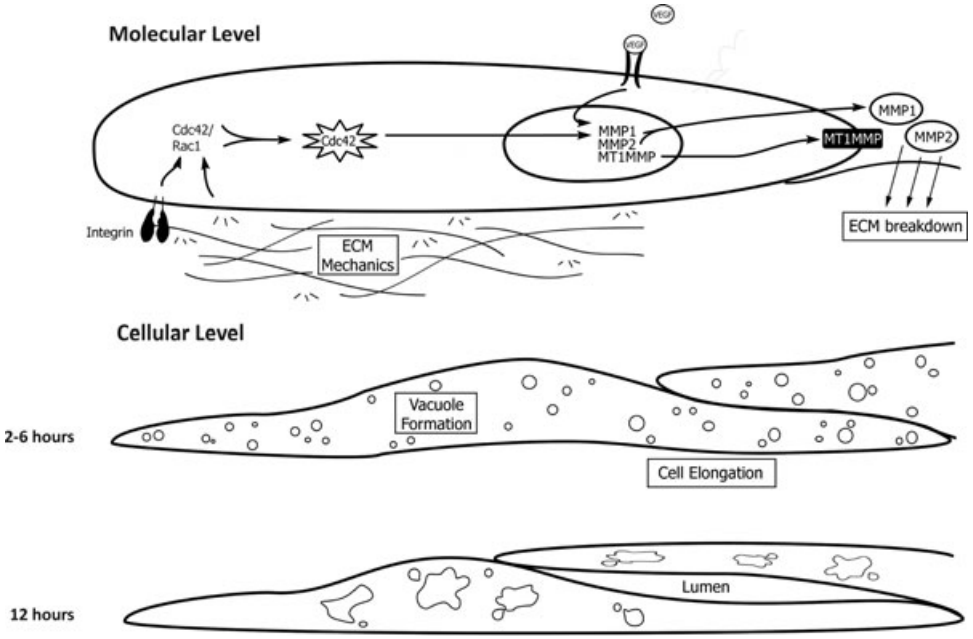

Fig. 6 Model for mechanics and VEGF co-regulation of tube morphogenesis (cellular and molecular level). VEGF initiates angiogenesis, with EPC assembly into a chain, by inducing MMP activation (upper panel), which further allows EPCs to elongate on substrate within 2–6 hrs (middle panel). Substrate mechanics activates Cdc42 (upper panel), resulting in intracellular vacuole formation (middle panel), extension and fusion to lumens after 12 hrs (middle and lower panels).

of stem cells [15, 16]. Biomechanical tension between ECs and the ECM has been demonstrated to regulate capillary development [11, 17, 21], in which mechanical forces exerted by the cells onto the surrounding ECM create pathways for migration that drive their migratory ability and their subsequent CLS formation [55, 56], as well as *in vivo* vascularization [23].

Hydrogels, which are structurally and mechanically similar to the native ECM of many tissues, have been utilized as a matrix to study cellular responses to mechanical stresses [16, 56, 57], as well as endothelial tubulogenesis [13, 58]. The body of evidence has shown that matrix stiffness modulates the ability of ECs to elongate and contract their surrounding ECM, suggesting that a reduced tension between the ECs and ECM is sufficient to trigger an intercellular signalling cascade leading to cellular movement and tubulogenesis [12, 13, 58, 59]. More recently, mechanical cues from the ECM and signals from growth factor receptors have been shown to regulate the balance of activity between TFII-I and GATA2, which govern the expression of VEGFR2, which, in turn, instigates angiogenesis [14]. However, the ECM elasticity range and optimum reported in these studies vary depending on the type of hydrogel (*e.g.* matrigel, collagen, polyacrylamide or self-assembly peptide), culture system (two-*versus* three-dimensional) and assay (*in vivo versus in vitro*) used in the study.

In the current study, utilizing chemically and mechanically defined hydrogels as an *in vitro* culture system for angiogenesis, we were able to study tube morphogenesis over a range of elasticity softer than usually available *in vitro* and relevant for vascular morphogenesis (10–650 Pa), as well as the response to growth factor administration. We have demonstrated that VEGF is a prerequisite for instigation of angiogenesis and that later progress in tube morphogenesis is regulated by mechanical stresses from the ECM (Fig. 6). First, MMP production induced by VEGF reduces the mechanical resistance of the ECM and allows EPC migration and reorganization. This MMP production is co-regulated by matrix stiffness, as EPCs cultured on the rigid and firm substrates have to produce more MMPs to overcome the extra mechanical barrier. At this stage, reduced elasticity of the ECM promotes tubulogenesis, which is characterized by a significant increase in mean tube length, tube area and thickness as matrix stiffness is reduced from rigid to yielding. Although EPCs cultured on rigid and firm substrates produce more MMPs, most likely to overcome the extra mechanical resistance, the local decrease in substrate stiffness cannot support predominant CLS formation. Hence, EPCs cultured on the yielding substrates are able to form predominant CLSs with extended vacuoles and open lumens.

Vessel morphogenesis is a highly dynamic process in which invasion, motility and lumenogenesis occur concurrently in different regions of the developing tube. In contrast to angiogenic sprouting, cell hollowing is a mechanism by which individual cells generate vacuoles through the pinocytosis process; these vacuoles then coalesce, forming a lumen that connects to the lumens of neighbouring cells [24, 25, 28, 29]. Here we observed that in response to VEGF and matrix stiffness, EPCs produce MMPs that allow further cellular migration and connection into CLSs (Fig. 2). Furthermore, we demonstrated the kinetics of CLS formation along 12 hrs (Fig. S2), vacuoles formation within 6 hrs (Fig. 4A) and enlarged vacuoles and lumens within 12 hrs (Fig. 4B).

Although *in vivo* and *in vitro* studies have shown that lumenal structures and tube formation involve the formation of intracellular vacuoles [25, 27], the molecular mechanisms of these processes have been delineated only recently. Using collagen as a

3D *in vitro* model of angiogenesis, Davis and colleagues showed that EC lumenization *via* formation and coalescence of pinocytic intracellular vacuole involves coordinated signalling pathways: localized at cell membranes, MT1-MMP degrades the ECM and creates a physical space to facilitate lumen formation [49, 50], while integrin–ECM interactions initiate a cascade of downstream signalling to activate the Rho GTPases Cdc42 and Rac1, which drive the formation of intracellular vacuoles [27].

We demonstrate that this molecular mechanism is co-regulated by both VEGF and ECM elasticity. MT1-MMP, which is present as an active enzyme on the cell surface, acts directly against different ECM proteins and can activate pro-MMPs at the cell surface, which localizes MMP activity to the pericellular area [48, 60]. We found that VEGF directly regulated the production of MT1-MMP, MMP-1 and MMP-2 in EPCs and further showed that the activity of MT1-MMP is required to initiate tube morphogenesis. Suppression of MT1-MMP mitigated CLS formation on the firm and yielding substrates while maintaining spreading on the rigid substrate. MT1-MMP suppressed EPCs were no longer able to degrade the surrounding ECM in order to form CLSs. On softer gels, where EPCs produced the least amount of MMPs and have dynamic adhesions [61], MT1-MMP suppression prevents them from spreading and causes them to exhibit a rounded morphology; on the rigid substrate, it allows EPCs to spread with a morphology similar to that exhibited when cultured in media with low levels of VEGF.

Downstream of integrin signalling, Cdc42 has been shown, using both *in vitro* and *in vivo* models, to mediate vascular morphogenesis events [25, 27]. We show that inhibition of Cdc42 prevented CLS formation on all substrates, regardless of elasticity. However, while the inhibition of Cdc42 does not prevent EPCs spreading on the rigid and firm substrates, they appear round on the yielding substrate. Suppression of Cdc42 prevents EPCs from physically resisting cell traction forces that are needed on the soft gel [56, 59], which result in rounded cell morphology on the yielding substrate. Furthermore, it was recently suggested that activated Cdc42 augmented MMP-2 and MT1-MMP activity [62], which supports our data that Cdc42 suppressed EPCs are unable to form CLSs on all substrates.

Acknowledgements

We thank Dr. Merv C. Yoder from the Indiana University School of Medicine for providing EPCs, Dr. Jennifer H. Elisseeff and Jeannine Coburn from JHU for assisting with microrheology measurements, and Michael McCaffery, Michelle Hussain and Ned Perkins from the Integrated Imaging Center at JHU for TEM processing and imaging, Steven Bolger from Duke University for assisting with real-time RT-PCR. This research was partially funded by an AHA-Scientist Development grant, National Institute of Health grant U54CA143868 and a March of Dimes-O'Conner Starter Scholar award (all for S.G.).

Conflict of interest disclosure

All authors declare no competing financial interests.

Supporting Information

Additional Supporting Information may be found in the online version of this article:

Fig. S1 Viscoelasticity of hydrogels. Microrheology measurements of HA:gelatin over 24 hrs of gelation show three distinct profiles of hydrogel mechanics: rigid, firm and yielding. Values shown are means ± S.D. for elastic modulus (G′) over 24 hrs during the *in situ* gelation.

Fig. S2 Time interval images of EPCs on rigid, firm and yielding substrates. Rapid chain assembly and CLS formation on softer substrates along the 12-hr culture period. Scale bar is 100 μm.

Fig. S3 RNAi for MT1-MMP and Cdc42. (**A**) Real-time RT-PCR analysis of siRNA transfected CB-EPCs shows significant suppression of MT1-MMP (left graph) or Cdc42 (right graph) compared to controls (Luciferase-transfected EPCs). Significance levels were set at $*P < 0.05$ and $***P < 0.001$, respectively. (**B**) Western blot analysis shows suppression of MT1-MMP (left panel) or Cdc42 (right panel) at protein level compared to Luciferase control. (**C**) Light microscope images of CB-EPCs transfected with Luciferase, MT1-MMP or Cdc42 seeded on rigid, firm and yielding substrates for 12 hrs. Scale bar is 100 μm.

Please note: Wiley-Blackwell are not responsible for the content or functionality of any supporting materials supplied by the authors. Any queries (other than missing material) should be directed to the corresponding author for the article.

References

1. **Asahara T, Murohara T, Sullivan A, *et al.*** Isolation of putative progenitor endothelial cells for angiogenesis. *Science*. 1997; 275: 964–7.
2. **Hill JM, Zalos G, Halcox JP, *et al.*** Circulating endothelial progenitor cells, vascular function, and cardiovascular risk. *N Engl J Med*. 2003; 348: 593–600.
3. **Takahashi T, Kalka C, Masuda H, *et al.*** Ischemia- and cytokine-induced mobilization of bone marrow-derived endothelial progenitor cells for neovascularization. *Nat Med*. 1999; 5: 434–8.
4. **Schatteman GC, Hanlon HD, Jiao C, *et al.*** Blood-derived angioblasts accelerate blood-flow restoration in

diabetic mice. *J Clin Invest*. 2000; 106: 571–8.

5. **Schächinger V, Assmus B, Britten MB, *et al.*** Transplantation of progenitor cells and regeneration enhancement in acute myocardial infarction: final one-year results of the TOPCARE-AMI trial. *J Am Coll Cardiol*. 2004; 44: 1690–9.
6. **Shepherd BR, Enis DR, Wang F, *et al.*** Vascularization and engraftment of a human skin substitute using circulating progenitor cell-derived endothelial cells. *FASEB J*. 2006; 20: 1739–41.
7. **Asahara T, Masuda H, Takahashi T, *et al.*** Bone marrow origin of endothelial progenitor cells responsible for postnatal vasculogenesis in physiological and pathological neovascularization. *Circ Res*. 1999; 85: 221–8.
8. **Li B, Sharpe EE, Maupin AB, *et al.*** VEGF and PlGF promote adult vasculogenesis by enhancing EPC recruitment and vessel formation at the site of tumor neovascularization. *FASEB J*. 2006; 20: 1495–7.
9. **Kaya D, Gürsoy-Özdemir Y, Yemisci M, *et al.*** VEGF protects brain against focal ischemia without increasing blood-brain permeability when administered intracerebroventricularly. *J Cereb Blood Flow Metab*. 2005; 25: 1111–8.
10. **Sun Y, Jin K, Xie L, *et al.*** VEGF-induced neuroprotection, neurogenesis, and angiogenesis after focal cerebral ischemia. *J Clin Invest*. 2003; 111: 1843–51.
11. **Davis GE, Senger DR.** Endothelial extracellular matrix: biosynthesis, remodeling, and functions during vascular morphogenesis and neovessel stabilization. *Circ Res*. 2005; 97: 1093–107.
12. **Deroanne CF, Lapiere CM, Nusgens BV.** In vitro tubulogenesis of endothelial cells by relaxation of the coupling extracellular matrix-cytoskeleton. *Cardiovasc Res*. 2001; 49: 647–58.
13. **Sieminski AL, Was AS, Kim G, *et al.*** The stiffness of three-dimensional ionic self-assembling peptide gels affects the extent of capillary-like network formation. *Cell Biochem Biophys*. 2007; 49: 73–83.
14. **Mammoto A, Connor KM, Mammoto T, *et al.*** A mechanosensitive transcriptional mechanism that controls angiogenesis. *Nature*. 2009; 457: 1103–8.
15. **McBeath R, Pirone DM, Nelson CM, *et al.*** Cell shape, cytoskeletal tension, and RhoA regulate stem cell lineage commitment. *Dev Cell*. 2004; 6: 483–95.
16. **Engler AJ, Sen S, Sweeney HL, *et al.*** Matrix elasticity directs stem cell lineage specification. *Cell*. 2006; 126: 677–89.
17. **Ingber DE, Folkman J.** Mechanochemical switching between growth and differentiation during fibroblast growth factor-stimulated angiogenesis in vitro: role of extracellular matrix. *J Cell Biol*. 1989; 109: 317–30.
18. **Matthews BD, Overby DR, Mannix R, *et al.*** Cellular adaptation to mechanical stress: role of integrins, Rho, cytoskeletal tension and mechanosensitive ion channels. *J Cell Sci*. 2006; 119: 508–18.
19. **Chen CS, Mrksich M, Huang S, *et al.*** Geometric control of cell life and death. *Science*. 1997; 276: 1425–8.
20. **Moore KA, Polte T, Huang S, *et al.*** Control of basement membrane remodeling and epithelial branching morphogenesis in embryonic lung by Rho and cytoskeletal tension. *Dev Dyn*. 2005; 232: 268–81.
21. **Davis GE, Camarillo CW.** Regulation of endothelial cell morphogenesis by integrins, mechanical forces, and matrix guidance pathways. *Exp Cell Res*. 1995; 216: 113–23.
22. **Ingber DE, Folkman J.** How does extracellular matrix control capillary morphogenesis? *Cell*. 1989; 58: 803–5.
23. **Kilarski WW, Samolov B, Petersson L, *et al.*** Biomechanical regulation of blood vessel growth during tissue vascularization. *Nat Med*. 2009; 15: 657–64.
24. **Lubarsky B, Krasnow MA.** Tube morphogenesis: making and shaping biological tubes. *Cell*. 2003; 112: 19–28.
25. **Kamei M, Brian SW, Bayless KJ, *et al.*** Endothelial tubes assemble from intracellular vacuoles in vivo. *Nature*. 2006; 442: 453–6.
26. **Folkman J, Haudenschild C.** Angiogenesis in vitro. *Nature*. 1980; 288: 551–6.
27. **Bayless KJ, Davis GE.** The Cdc42 and Rac1 GTPases are required for capillary lumen formation in three-dimensional extracellular matrices. *J Cell Sci*. 2002; 115: 1123–36.
28. **Davis GE, Camarillo CW.** An $\alpha 2\beta 1$ integrin-dependent pinocytic mechanism involving intracellular vacuole formation and coalescence regulates capillary lumen and tube formation in three-dimensional collagen matrix. *Exp Cell Res*. 1996; 224: 39–51.
29. **Iruela-Arispe ML, Davis GE.** Cellular and molecular mechanisms of vascular lumen formation. *Dev Cell*. 2009; 16: 222–31.
30. **Collen A, Hanemaaijer R, Lupu F, *et al.*** Membrane-type matrix metalloproteinase-mediated angiogenesis in a fibrin-collagen matrix. *Blood*. 2003; 101: 1810–7.
31. **Gálvez BG, Matías-Román S, Albar JP, *et al.*** Membrane type 1-matrix metalloproteinase is activated during migration of human endothelial cells and modulates endothelial motility and matrix remodeling. *J Biol Chem*. 2001; 276: 37491–500.
32. **Romanic AM, White RF, Arleth AJ, *et al.*** Matrix metalloproteinase expression increases after cerebral focal ischemia in rats: inhibition of matrix metalloproteinase-9 reduces infarct size. *Stroke*. 1998; 29: 1020–30.
33. **Galis ZS, Sukhova GK, Lark MW, *et al.*** Increased expression of matrix metalloproteinases and matrix degrading activity in vulnerable regions of human atherosclerotic plaques. *J Clin Invest*. 1994; 94: 2493–503.
34. **Ingram DA, Mead LE, Tanaka H, *et al.*** Identification of a novel hierarchy of endothelial progenitor cells using human peripheral and umbilical cord blood. *Blood*. 2004; 104: 2752–60.
35. **Yoder MC, Mead LE, Prater D, *et al.*** Redefining endothelial progenitor cells via clonal analysis and hematopoietic stem/progenitor cell principals. *Blood*. 2007; 109: 1801–9.
36. **Mead LE, Prater D, Yoder MC, *et al.*** Isolation and characterization of endothelial progenitor cells from human blood. *Curr Protoc Stem Cell Biol*. 2008; 2: 2C.1.
37. **Prater DN, Case J, Ingram DA, *et al.*** Working hypothesis to redefine endothelial progenitor cells. *Leukemia*. 2007; 21: 1141–9.
38. **Timmermans F, Plum J, Yöder MC, *et al.*** Endothelial progenitor cells: identity defined? *J Cell Mol Med*. 2009; 13: 87–102.
39. **Vanderhooft JL, Alcoutlabi M, Magda JJ, *et al.*** Rheological properties of cross-linked hyaluronan-gelatin hydrogels for tissue engineering. *Macromol Biosci*. 2009; 9: 20–8.
40. **Boudou T, Ohayon J, Picart C, *et al.*** An extended relationship for the characterization of Young's modulus and Poisson's ratio of tunable polyacrylamide gels. *Biorheology*. 2006; 43: 721–8.
41. **Perkins EM, McCaffery JM.** Conventional and immunoelectron microscopy of mitochondria. *Methods Mol Biol*. 2007; 372: 467–83.
42. **Shu XZ, Ahmad S, Liu Y, *et al.*** Synthesis and evaluation of injectable, in situ crosslinkable synthetic extracellular matrices for tissue engineering. *J Biomed Mater Res* A. 2006; 79: 902–12.
43. **Gerecht S, Burdick JA, Ferreira LS, *et al.*** Hyaluronic acid hydrogel for controlled

self-renewal and differentiation of human embryonic stem cells. *Proc Natl Acad Sci USA*. 2007; 104: 11298–303.

44. **Au P, Daheron LM, Duda DG, *et al.*** Differential *in vivo* potential of endothelial progenitor cells from human umbilical cord blood and adult peripheral blood to form functional long-lasting vessels. *Blood*. 2008; 111: 1302–5.
45. **Bettinger CJ, Zhang Z, Gerecht S, *et al.*** Enhancement of *in vitro* capillary tube formation by substrate nanotopography. *Adv Mater*. 2008; 20: 99–103.
46. **Hirschi KK, Ingram DA, Yoder MC.** Assessing identity, phenotype, and fate of endothelial progenitor cells. *Arterioscler Thromb Vasc Biol*. 2008; 28: 1584–95.
47. **Ferreira LS, Gerecht S, Shieh HF, *et al.*** Vascular progenitor cells isolated from human embryonic stem cells give rise to endothelial and smooth muscle like cells and form vascular networks *in vivo*. *Circ Res*. 2007; 101: 286–94.
48. **Van Hinsbergh VWM, Engelse MA, Quax PHA.** Pericellular proteases in angiogenesis and vasculogenesis. *Arterioscler Thromb Vasc Biol*. 2006; 26: 716–28.
49. **Chun TH, Sabeh F, Ota I, *et al.*** MT1-MMP-dependent neovessel formation within the confines of the three-dimensional extracellular matrix. *J Cell Biol*. 2004; 167: 757–67.
50. **Saunders WB, Bohnsack BL, Faske JB, *et al.*** Coregulation of vascular tube stabilization by endothelial cell TIMP-2 and pericyte TIMP-3. *J Cell Biol*. 2006; 175: 179–91.
51. **Jaffe AB, Hall A.** Rho GTPases: biochemistry and biology. *Annu Rev Cell Dev Biol*. 2005; 21: 247–69.
52. **Mammoto A, Mammoto T, Ingber DE.** Rho signaling and mechanical control of vascular development. *Curr Opin Hematol*. 2008; 15: 228–34.
53. **Aicher A, Zeiher AM, Dimmeler S.** Mobilizing endothelial progenitor cells. *Hypertension*. 2005; 45: 321–5.
54. **Urbich C, Dimmeler S.** Endothelial progenitor cells: characterization and role in vascular biology. *Circ Res*. 2004; 95: 343–53.
55. **Lo CM, Wang HB, Dembo M, *et al.*** Cell movement is guided by the rigidity of the substrate. *Biophys J*. 2000; 79: 144–52.
56. **Discher DE, Janmey P, Wang Y-l.** Tissue cells feel and respond to the stiffness of their substrate. *Science*. 2005; 310: 1139–43.
57. **Ghosh K, Pan Z, Guan E, *et al.*** Cell adaptation to a physiologically relevant ECM mimic with different viscoelastic properties. *Biomaterials*. 2007; 28: 671–9.
58. **Sieminski AL, Hebbel RP, Gooch KJ.** The relative magnitudes of endothelial force generation and matrix stiffness modulate capillary morphogenesis *in vitro*. *Exp Cell Res*. 2004; 297: 574–84.
59. **Ingber DE.** Mechanical signaling and the cellular response to extracellular matrix in angiogenesis and cardiovascular physiology. *Circ Res*. 2002; 91: 877–87.
60. **Haas TL.** Endothelial cell regulation of matrix metalloproteinases. *Can J Physiol Pharmacol*. 2005; 83: 1–7.
61. **Pelham Jr RJ, Wang YL.** Cell locomotion and focal adhesions are regulated by substrate flexibility. *Proc Natl Acad Sci USA*. 1997; 94: 13661–5.
62. **Ispanovic E, Serio D, Haas TL.** Cdc42 and RhoA have opposing roles in regulating membrane type 1-matrix metalloproteinase localization and matrix metalloproteinase-2 activation. *Am J Physiol Cell Physiol*. 2008; 295: C600–10.